

# COMPARING DETRITAL AGE SPECTRA, AND OTHER GEOLOGICAL DISTRIBUTIONS, USING THE WASSERSTEIN DISTANCE

SUBMITTED, NON-PEER REVIEWED MANUSCRIPT, COMPILED OCTOBER 26, 2022

Alex G. Lipp<sup>1</sup> and Pieter Vermeesch<sup>2</sup>

<sup>1</sup>Merton College, University of Oxford, Oxford, UK

<sup>2</sup>Department of Earth Sciences, University College London, London, UK

## ABSTRACT

Distributional data such as detrital age populations or grain size distributions are common in the geological sciences. As analytical techniques become more sophisticated, increasingly large amounts of distributional data are being gathered. These advances require quantitative and objective methods, such as multidimensional scaling (MDS), to analyse large numbers of samples. Crucial to such methods is choosing a sensible measure of dissimilarity between samples. At present, the Kolmogorov-Smirnov (KS) statistic is the most widely used of these dissimilarity measures. However, the KS statistic has some limitations. It is very sensitive to differences between the modes of two distributions, and relatively insensitive to differences between their tails. Here we introduce the Wasserstein-2 distance ( $W_2$ ) as an alternative to address this issue. Whereas the KS-distance is defined as the maximum vertical distance between two empirical cumulative distribution functions, the  $W_2$ -distance is a function of the horizontal distances (i.e., age differences) between individual observations. Using a combination of synthetic examples and a published zircon U-Pb dataset, we show that the  $W_2$  distance produces similar MDS results to the KS-distance in most cases, but significantly different results in some cases. Where the results differ, the  $W_2$  results are geologically more sensible. For the case study, we find that the MDS map that is produced using  $W_2$  can be readily interpreted in terms of the shape and average age of the age spectra. The  $W_2$ -distance has been added to the R package `IsoplotR`, for immediate use in detrital geochronology and other applications. The  $W_2$  distance can be generalised to multiple dimensions, which opens opportunities beyond distributional data.

**Keywords** Distributional data · Wasserstein distance · Kolmogorov-Smirnov distance · Detrital mineral ages · Zircon U-Pb dating · Multi-dimensional scaling

## 1 INTRODUCTION

A distributional dataset is one where the information does not lie in individual observations, but in the *distribution* of many observations associated with one sample. Such data are common in the geological sciences, for example, detrital mineral ages or grain size distributions. Zircon U-Pb ages, in igneous and detrital samples, are one particularly widely used class of distributional data, which are used *inter alia* to constrain sediment provenance, global magmatic processes, and the evolution of plate tectonics (e.g., Condie et al. 2009; Cawood et al. 2012; Reimink et al. 2021). Analytical advances mean that we require objective and quantitative ways to analyse increasingly large amounts of distributional data. Qualitative comparison becomes infeasible when even modest numbers of samples are being analysed. For example, the dimension reducing technique of multi-dimensional scaling (MDS) has become popular for analysing large numbers of detrital age spectra simultaneously (Vermeesch 2013; Sharman et al. 2018). This method, and others, require a dissimilarity metric between samples to be specified (Vermeesch 2018a). Such a metric corresponds to how ‘different’ two distributional samples are. The choice of metric is vital as different metrics can result in different MDS ‘maps’ and potentially different geological interpretations.

The Kolmogorov-Smirnov (KS) distance, calculated as the maximum vertical distance between two empirical cumulative distribution functions (ECDFs) has emerged as a ‘canonical’ distance metric between mineral age distributions (Berry et al. 2001;

Vermeesch 2018a). However, the KS-distance has a number of drawbacks, chiefly that as only the *maximum* vertical difference between ECDFs is important, it is insensitive to variability in the tails of distributions. A number of alternative dissimilarity measures have previously been proposed to address this issue, including established methods such as the Kuiper statistic, and ad-hoc dissimilarity measures such as the ‘likeness’ and ‘cross-correlation’ coefficients (Saylor et al. 2012; Satkoski et al. 2013; Sharman et al. 2018). Unfortunately, all these alternatives have drawbacks, including a propensity for the ad-hoc dissimilarity measures to produce unintuitive results when applied to extremely large and/or precise datasets (Vermeesch 2018a).

In this paper we present an alternative to the KS-distance that does not suffer from these drawbacks: the Wasserstein distance (also known as the Earth-mover’s or Kantorovich–Rubinstein distance). To introduce the chief principle behind this measure, let us consider a simple toy example. Table 1 contains four samples (A through D), each of which contains exactly one single grain analysis:

Table 1: A toy, single-grain per sample dataset

Sample	A	B	C	D
Age, Ma	1	1	2	11

As the KS distance is the vertical difference between ECDFs, it is insensitive to the absolute, ‘horizontal’ age differences between

\*correspondence: alexander.lipp@merton.ox.ac.uk

individual observations. Thus, the KS-distances between  $A$  and the other three samples are  $KS(A, B) = 0$ ,  $KS(A, C) = 1$  and  $KS(A, D) = 1$ . Counter to our expectation, the KS-distance cannot ‘see’ the relative age difference between sample  $A$  and samples  $C$  and  $D$ . For the toy example, the Wasserstein distance simply corresponds to the horizontal distance between the four samples. Thus,  $W(A, B) = 0$ ,  $W(A, C) = 1$ , and  $W(A, D) = 10$ , which is a more sensible result than that achieved with the KS-distance.

In the following sections, we first introduce the Wasserstein distance in a more realistic setting, and formally define it. Next we discuss how it can be decomposed into intuitive terms that accord with how qualitatively, as geologists, we might compare distributions. We then proceed to compare the Wasserstein distance to the KS distance using a simple yet realistic synthetic example. Finally, we perform a case study, analysing eight real zircon U-Pb age spectra from Scandinavian river sediments using MDS with the Wasserstein distance. Whilst we focus primarily on detrital age distributions, we emphasise that much of the following discussion applies equally to any form of distributional data.

## 2 THE WASSERSTEIN DISTANCE

The Wasserstein distance is a distance metric between two probability measures from a branch of mathematics called ‘optimal transport’. Optimal transport is often intuited in terms of moving piles of sand from one location to another with no loss or gain of material (e.g., Villani 2003). The problem that optimal transport solves is finding the way to transport the sand such that least sand is moved the least distance. The Wasserstein distance is the cost associated with this most efficient transportation. The association with moving piles of sand is why the Wasserstein distance is often termed the Earth-mover’s distance. Figure 1a shows an example of how one univariate probability distribution,  $\mu$ , based on a detrital age spectrum, is transformed into another,  $\nu$  according to the optimal transport plan. Like the KS-distance the Wasserstein defines a metric space, satisfying the triangle inequality. Elsewhere in the Earth sciences, the Wasserstein distance is increasingly being used for solving non-linear geophysical inverse problems (e.g., Engquist and Froese 2014; Métivier et al. 2016; Sambridge et al. 2022). Full mathematical treatments of the Wasserstein distance and optimal transport are beyond the scope of this paper, but interested readers are referred to Villani (2003) or Peyré and Cuturi (2019). A geophysical perspective is given in Sambridge et al. (2022).

### 2.1 Formal definition

We consider two univariate probability distributions  $\mu$  and  $\nu$  which have cumulative distribution functions (CDFs)  $M$  and  $N$  respectively. The  $p^{\text{th}}$  Wasserstein distance between  $\mu$  and  $\nu$  is given by:

$$W_p(\mu, \nu) = \left( \int_0^1 |M^{-1} - N^{-1}|^p dt \right)^{1/p}. \quad (1)$$

where  $M^{-1}$  indicates the inverse of the CDF  $M$  and  $0 \leq t \leq 1$  (Villani 2003). Note that this definition of  $W_p$  assumes that the cost-function is given by  $|x - y|^p$  (e.g., the Euclidean distance where  $p = 2$ ), which is the case for most distributional data

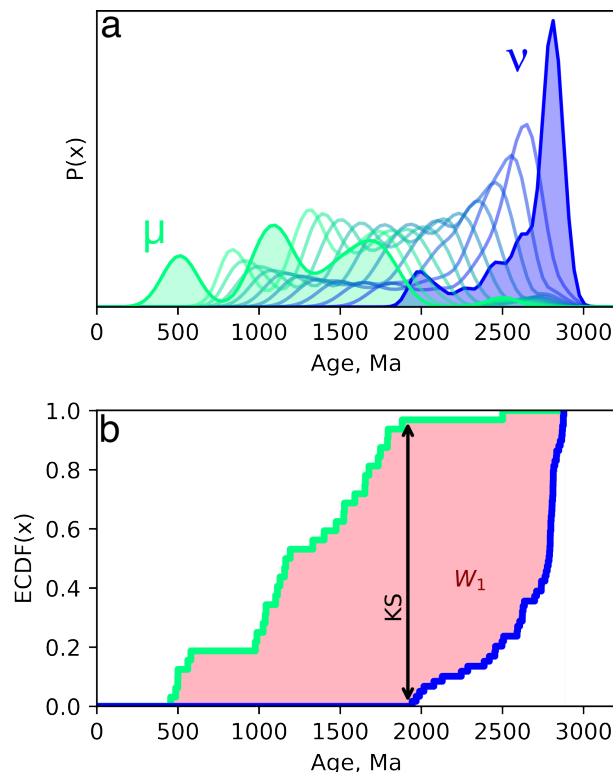


Figure 1: **Intuition of the Wasserstein distance.** a) Green and blue filled polygons show two example probability distributions of mineral ages from two samples. The distributions are labelled  $\mu$  and  $\nu$  for consistency with Equation 1. Semi-transparent coloured lines are probability distributions spaced equally in Wasserstein space between  $\mu$  and  $\nu$  (termed ‘barycentres’; Benamou et al. 2015). b) Empirical Cumulative Distribution Functions (ECDFs) of the detrital ages used to calculate the distributions shown in panel a, same colours. The first Wasserstein ( $W_1$ ) distance corresponds to the total area between the two ECDFs (shaded pink). The Kolmogorov-Smirnov (KS) distance is the maximum distance between the two ECDFs (black double-headed arrow). The data used to generate these distributions is taken from the ‘Byskealven’ and ‘Vefsna’ samples of Morton et al. (2008), but modified to aid illustration.

in geology. In the further special case of  $p = 1$  (i.e., the *first* Wasserstein distance,  $W_1$ ), Equation 1 can be re-written simply as:

$$W_1(\mu, \nu) = \int_x |M - N| dx, \quad (2)$$

which is the area between two CDFs (e.g., Figure 1b). Recall that the KS-distance between two distributions is the maximum distance between the two corresponding CDFs. Whilst the  $W_1$  is easily visualised, we actually use the  $W_2$  going forwards as the *squared* distance (i.e.,  $p = 2$ ) between observations is the standard distance metric in most statistical analyses (e.g., least squares regression). Additionally,  $W_2$  decomposes into readily interpretable terms, as discussed below.

We focus on these univariate instances as they apply to the most common geological distributional data including detrital age distributions and grain size distributions. However, we note that the Wasserstein distance is, in general, multivariate. As a

result, some form of the Wasserstein distance could prove useful for analysing a number of other geological datasets such as the geochemical compositions of detrital minerals, or joint U-Pb and Lu-Hf isotope analysis. Statistics for comparing distributional data in multiple dimensions are increasingly needed (Sundell and Saylor 2021).

A property of the KS-distance is that it is insensitive to whether the data are presented as ‘raw’ or log-transformed ages. This property arises as the KS-distance is only sensitive to the relative ordering of observations in a distribution, which is insensitive to a log transformation. The  $W_2$  however will give different results depending on whether the data are transformed or not. For the remainder of this study we consider only raw ages, focussing as a result on *absolute* age differences. However, we can conceive of situations in which it is *relative* age differences which are of interest, in which case a logarithmic transformation would be applied prior to calculating  $W_2$ .

## 2.2 Decomposition

A particularly useful property of  $W_2$  between two univariate distributions is that it can be decomposed in terms of the differences between the two distributions’ location, spread and shape. Irpino and Romano 2007 show that:

$$W_2^2(\mu, \nu) = \underbrace{(\bar{\mu} - \bar{\nu})^2}_{\text{Location}} + \underbrace{(\sigma_\mu - \sigma_\nu)^2}_{\text{Spread}} + \underbrace{2\sigma_\mu\sigma_\nu(1 - \rho^{\mu\nu})}_{\text{Shape}}, \quad (3)$$

where  $\bar{\mu}$  is the mean of  $\mu$ ,  $\sigma_\mu$  is the standard deviation of  $\mu$  and  $\rho^{\mu\nu}$  is the Pearson correlation coefficient between the quantiles of the distributions  $\mu$  and  $\nu$ . These three terms also accord with, qualitatively, how as geologists we might compare two distributions.

## 2.3 Discrete data

Most distributional data in the Earth sciences do not, in raw form, follow continuous probability distributions. Instead, samples may be discrete sets of observations, e.g., lists of individual mineral ages. The above formulations can be easily applied to such cases by describing the probability functions  $\mu$  and  $\nu$  as weighted sums of  $\delta$  functions. For example, let us consider two samples  $x_m$  and  $x_n$  with  $p$  and  $q$  numbers of observations respectively:

$$\mu = \sum_i^p m_i \delta_{x_m}, \quad \nu = \sum_i^q n_i \delta_{x_n} \quad (4)$$

where  $m$  and  $n$  are weight vectors, such that  $\sum m = \sum n = 1$ . In most geological cases these weights would be uniform,  $m_i = 1/p$ ;  $n_i = 1/q$ , giving each observation within a sample equal weight. In this scenario,  $M$  and  $N$  are the familiar empirical cumulative distribution functions (ECDF), given as a series of step functions (e.g., Figure 1b).

## 3 SYNTHETIC DATA

We consider two probability density functions of mineral ages: a bimodal distribution and a unimodal distribution, both constructed from Gaussians with the same scale (Figure 2a). We fix

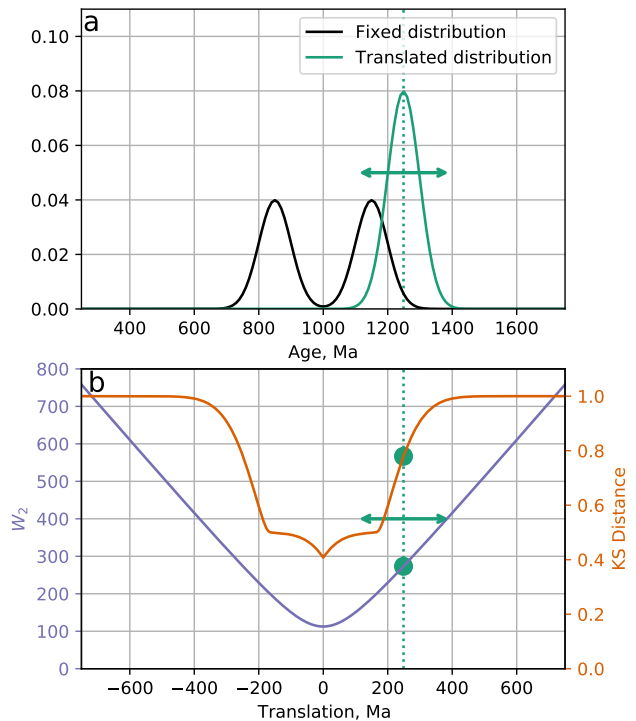


Figure 2: **Comparing the Wasserstein distance to the Kolmogorov-Smirnov distance.** a) Two synthetic probability density functions, modelled on U-Pb age spectra. The black bimodal distribution is fixed at 1000 Ma, and the green unimodal distribution is translated along the time axis. b) For each translated distribution, we calculate the KS-distance (red line) and  $W_2$  (blue line). The green dashed line and circles indicate values associated with the location of the green distribution shown in panel a.

the bimodal distribution at 1000 Ma, but translate the unimodal distribution along the time axis. For each translated distribution we calculate both the KS-distance and  $W_2$ . Figure 2b displays the behaviour of both distances under this scenario. The KS-distance shows an unexpectedly complex response containing a series of steps, as the peaks of the distributions align and misalign. At around  $\pm 400$  Ma, once the distributions stop overlapping, the KS-distance plateaus at its maximum value of 1. By contrast,  $W_2$  increases monotonically with increasing distance. Away from the origin,  $W_2$  approximates a linear function of the amount of translation, as is predicted from Equation 3. At the origin, the non-zero value of  $W_2$  is the cost of turning the unimodal distribution into the bimodal distribution without translation.

We argue that the behaviour of  $W_2$  is more geologically intuitive than the KS-distance under this scenario. It is useful geological information if two distributions differ in their means by 400, 500 or 1000 Ma, but if the distributions do not overlap, the KS-distance is insensitive to this. The Wasserstein distance

Table 2: The geological provinces drained by each of the rivers sampled in Morton et al. (2008), reproduced from Table 1 of the original study.

Sample	Geological Province
Byskealven	Fennoscandian Shield
Ranealven	Fennoscandian Shield
Lainioalven	Archaean
Ljusnan	Trans Scandinavian Igneous Belt
Salteva	Norwegian Caledonides
Vefsna	Norwegian Caledonides
Vindelalven	Swedish Caledonides
Ljungan	Swedish Caledonides

is, by contrast, sensitive to the absolute offset between non-overlapping distributions. Additionally, the stepped response of the KS-distance under translation is undesirable. Under the simple operation of translating a unimodal distribution, we would expect our dissimilarity to increase at a constant, or at least predictable (e.g., quadratic) rate. The change of the KS-distance with translation is, unintuitively, non-linear. By contrast, the  $W_2$  increases linearly with respect to translation.

#### 4 USE OF WASSERSTEIN DISTANCE IN MDS

We now use  $W_2$  to analyse a real dataset of zircon U-Pb ages from Scandinavian river sediments gathered by Morton et al. (2008). This dataset contains eight samples displayed as kernel density estimates in Figure 3a–h and ECDFs in Figure 3i. The data required to reproduce our results is provided in .csv format at the code repository (<https://github.com/AlexLipp/detrital-wasserstein/>). The primary geological province in each sample’s drainage basin is shown in Table 2. Here, we use MDS to jointly compare all samples (Vermeesch 2013). One of the desirable properties of the Wasserstein distance is that it fulfils the metric requirements, just like the KS-distance (Villani 2003). Therefore,  $W_2$  dissimilarity measures can be analysed by classical as well as non-metric MDS algorithms (Vermeesch 2013). The MDS ‘maps’ calculated by non-metric MDS, using both  $W_2$  and the KS-distance, are shown in Figure 3j–k. We investigate whether the KS map or the  $W_2$  map shows greater geological meaning.

We initially focus on two samples: Ranealven (Figure 3a) and Ljusnan (Figure 3d). These two samples have very similar distribution shapes with one prominent peak, and a smaller younger peak. However, the prominent peak is slightly offset between the two distributions such that there is little overlap. This feature is well shown in the ECDF plot in Figure 3h. As there is limited overlap between them, the KS-distance between these two visually similar distributions approaches its maximum value of 1. As a result, when MDS is applied to the dataset using the KS-distance these two samples are, counter-intuitively, widely separated (Figure 3k). By contrast, when using  $W_2$ , the samples are close together (Figure 3j).

The  $W_2$  MDS projection also accords well with the actual geological provenance of these samples (Table 2), with samples of the same provenance being grouped together. Whilst the axes of an MDS plot hold no inherent meaning, we can interpret relative positions on the map in terms of distributions’ shapes

and average ages. The horizontal axis, in this case, appears approximately coincident with the average age of the samples, with the samples to the left being generally older than those on the right. For example, the peak of Ljusnan is younger than that of Ranealven. In addition, the sample containing the most recent grains, Vefsna, is the furthest to the right. Contrastingly, Lainioalven, which uniquely drains Archean rocks, is the furthest to the left. Similarly, the vertical axis correlates approximately with distribution shape. Salteva & Vefsna have a broad, multimodal distribution and are placed towards the bottom of the map. Conversely, Ranealven & Ljusnan are largely unimodal. Byskealven & Vindelalven lie between these two endmembers and this is reflected in the MDS map. Given that  $W_2$  can be deconvolved into interpretable statistics (Equation 3) it is not surprising that the MDS maps produced can also be discussed in these terms.

#### 5 IMPLEMENTATION

We provide example code in both python and R that calculates  $W_2$  between two univariate distributions (U-Pb zircon ages) using the analytical expression above (Equation 1). In R, the  $W_2$ -distance has been added to the `IsoplotR` package (Vermeesch 2018b). This software can either be accessed using an (online) graphical user interface, at<sup>2</sup> <https://pieter-vermeesch.es.ucl.ac.uk/isoplotr/>. Alternatively, the function can also be accessed from the command line<sup>3</sup>:

```
# load the package:
library(IsoplotR)
DZ <- read.data("scandinavia.csv",method="detritals")
# example 1. calculate the W2 distance matrix for
# the Scandinavian dataset:
d <- diss(DZ,method="W2")
# example 2. apply MDS to the Scandinavian data set:
mds(DZ,method="W2")
```

In python, we make use of the POT package to calculate  $W_2$  (Flamary et al. 2021). The following snippet calculates  $W_2$  between the Byskealven and Vefsna age distribution from the example above. The data required, and a python script, is provided at <https://github.com/AlexLipp/detrital-wasserstein/>:

```
# Load in the packages
import numpy as np
import ot
# Load data
vefsna = np.loadtxt("vefsna.csv",delimiter=",",skiprows=1)
byskealven = np.loadtxt("byskealven.csv",delimiter=",",
                        skiprows=1)
# Calculate W_2^2 between vefsna and byskealven samples
W2_2 = ot.wasserstein_1d(vefsna,byskealven,p=2)
# Calculate W2 using square root
W2 = np.sqrt(W2_2)
```

The above code returns a  $W_2$  of 490.01.

<sup>2</sup>This is a temporary URL pointing to the beta version of the software. This will be replaced with a link to the public `IsoplotR` mirror once the review process has been completed.

<sup>3</sup>To install the beta version of the `IsoplotR` package, enter `remotes::install_github("pvermeesch/IsoplotRbeta")` in the R console

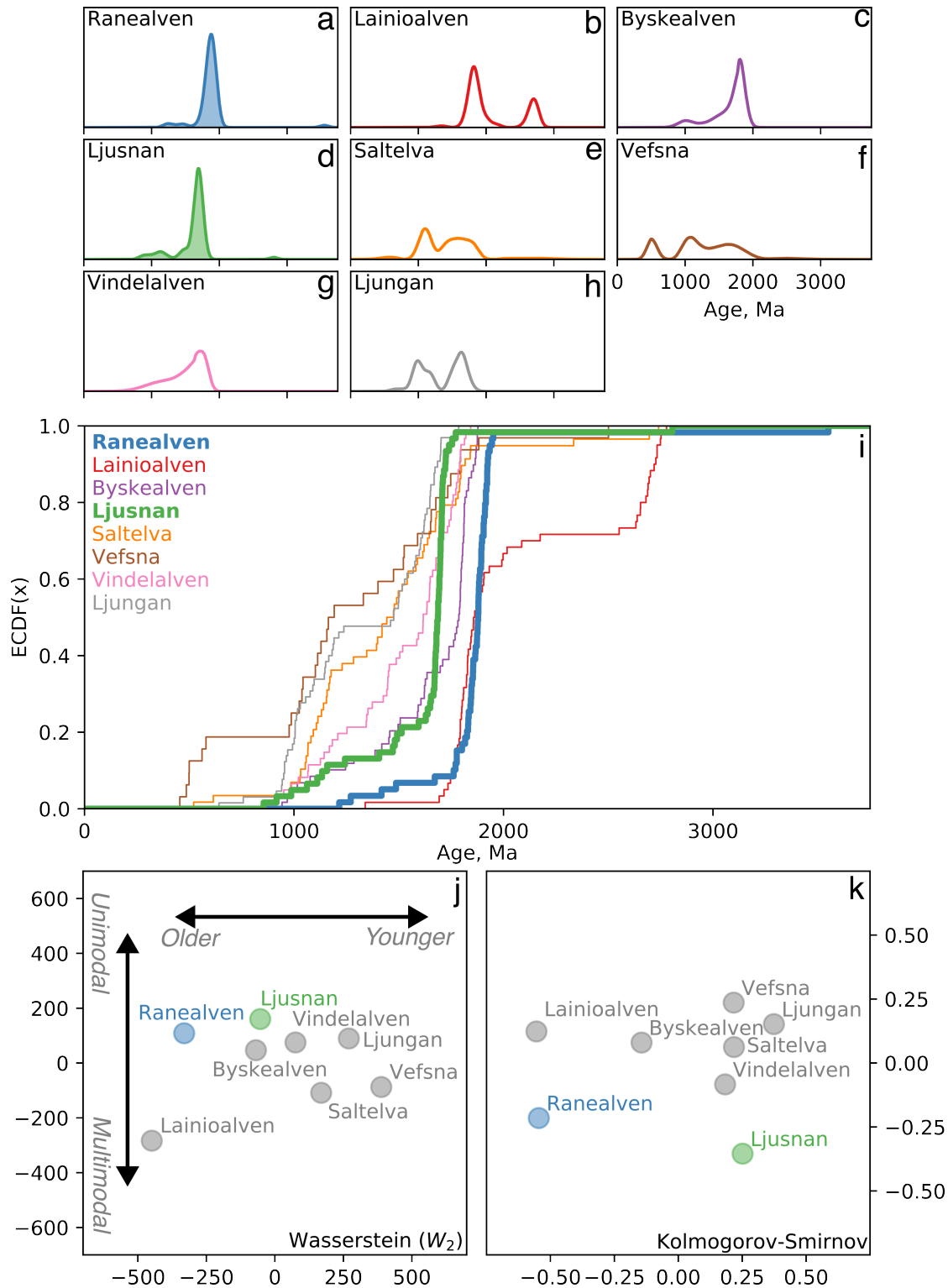


Figure 3: **Analysing detrital zircon U-Pb ages using the Wasserstein distance.** a–h) Kernel Density Estimates (KDEs) of zircon U-Pb ages from modern sand gathered in Scandinavian rivers by Morton et al. (2008). Sampled river names are indicated in the upper left corners of the plots. ‘Ranealven’ and ‘Ljusnan’ samples are filled in and highlighted in panels i–k. KDEs generated using a Gaussian kernel with adaptive bandwidth (Shimazaki and Shinomoto 2010). i) Empirical Cumulative Distribution Functions (ECDFs) for each zircon age population. j) Multi-Dimensional Scaling (MDS) map for zircon populations calculated using  $W_2$  as a dissimilarity metric. Note the closeness of ‘Ranealven’ and ‘Ljusnan’. k) MDS map of same samples but using KS-distance. Note the distance separating ‘Ranealven’ and ‘Ljusnan’.

## 6 CONCLUSIONS

The second Wasserstein distance,  $W_2$ , is an effective metric for comparing distributional data in the geological sciences such as detrital age spectra or grain size. The metric is particularly useful for univariate data, but can be extended to further dimensions.  $W_2$  is a function of the horizontal distances between observations, in contrast to the KS distance, which corresponds to vertical differences between ECDFs. Consequently, unlike the KS-distance,  $W_2$  is sensitive to variability in the tails of distributions, not just the modes. Under synthetic tests we find that the  $W_2$  metric behaves more intuitively in comparing distributions relative to the KS-distance. We performed a case study in which eight zircon U-Pb age distributions from Scandinavian river sediments were analysed by MDS using  $W_2$ . We showed that the resulting MDS map accurately clusters samples with the same provenance together. Additionally, the relative positions of samples on the map coincide with trends in interpretable qualities such as distribution shape and average age. The univariate  $W_2$  distance has an analytical solution, which we provide implementations of in R and python for detrital geochronology and other Earth science applications.

## ACKNOWLEDGEMENTS

AGL is funded by a Junior Research Fellowship from Merton College, Oxford. PV is supported by NERC Standard Grant #NE/T001518/1. This work benefited from discussions with Malcolm Sambridge & Kerry Gallagher.

## REFERENCES

- Benamou, J.-D., G. Carlier, M. Cuturi, L. Nenna, and G. Peyré (2015). “Iterative Bregman Projections for Regularized Transportation Problems”. *SIAM Journal on Scientific Computing* 2.37, A1111–A1138. doi: [10.1137/141000439](https://doi.org/10.1137/141000439).
- Berry, R. F., G. A. Jenner, S. Meffre, and M. N. Tubrett (2001). “A North American provenance for Neoproterozoic to Cambrian sandstones in Tasmania?” *Earth and Planetary Science Letters* 192.2, pp. 207–222. doi: [10.1016/S0012-821X\(01\)00436-8](https://doi.org/10.1016/S0012-821X(01)00436-8).
- Cawood, P., C. Hawkesworth, and B. Dhuime (2012). “Detrital zircon record and tectonic setting”. *Geology* 40.10, pp. 875–878. doi: [10.1130/G32945.1](https://doi.org/10.1130/G32945.1).
- Condie, K. C., E. Belousova, W. L. Griffin, and K. N. Sircombe (2009). “Granitoid events in space and time: Constraints from igneous and detrital zircon age spectra”. *Gondwana Research. Special Issue: Supercontinent Dynamics* 15.3, pp. 228–242. doi: [10.1016/j.gr.2008.06.001](https://doi.org/10.1016/j.gr.2008.06.001).
- Engquist, B. and B. D. Froese (2014). “Application of the Wasserstein metric to seismic signals”. *Communications in Mathematical Sciences* 12.5, pp. 979–988. doi: [10.4310/CMS.2014.v12.n5.a7](https://doi.org/10.4310/CMS.2014.v12.n5.a7).
- Flamary, R., N. Courty, A. Gramfort, M. Z. Alaya, A. Boisbunon, S. Chambon, L. Chapel, A. Corenflos, K. Fatras, N. Fournier, L. Gautheron, N. T. H. Gayraud, H. Janati, A. Rakotomamonjy, I. Redko, A. Rolet, A. Schutz, V. Seguy, D. J. Sutherland, R. Tavenard, A. Tong, and T. Vayer (2021). “POT: Python Optimal Transport”. *Journal of Machine Learning Research* 22.78, pp. 1–8.
- Irpino, A. and E. Romano (2007). “Optimal histogram representation of large data sets: Fisher vs piecewise linear approximation”. *Actes des cinquièmes journées Extraction et Gestion des Connaissances. Extraction et gestion des connaissances (2007). Vol. E-9. Namur, Belgium*, pp. 99–110.
- Métivier, L., R. Brossier, Q. Mérigot, E. Oudet, and J. Virieux (2016). “An optimal transport approach for seismic tomography: application to 3D full waveform inversion”. *Inverse Problems* 32.11, p. 115008. doi: [10.1088/0266-5611/32/11/115008](https://doi.org/10.1088/0266-5611/32/11/115008).
- Morton, A., M. Fanning, and P. Milner (2008). “Provenance characteristics of Scandinavian basement terrains: Constraints from detrital zircon ages in modern river sediments”. *Sedimentary Geology* 210.1, pp. 61–85. doi: [10.1016/j.sedgeo.2008.07.001](https://doi.org/10.1016/j.sedgeo.2008.07.001).
- Peyré, G. and M. Cuturi (2019). “Computational Optimal Transport”. *Foundations and Trends in Machine Learning* 11.5, pp. 355–607.
- Reimink, J. R., J. H. F. L. Davies, and A. Ielpi (2021). “Global zircon analysis records a gradual rise of continental crust throughout the Neoproterozoic”. *Earth and Planetary Science Letters* 554, p. 116654. doi: [10.1016/j.epsl.2020.116654](https://doi.org/10.1016/j.epsl.2020.116654).
- Sambridge, M., A. Jackson, and A. P. Valentine (2022). “Geophysical inversion and optimal transport”. *Geophysical Journal International* 231.1, pp. 172–198. doi: [10.1093/gji/ggac151](https://doi.org/10.1093/gji/ggac151).
- Satkoski, A. M., B. H. Wilkinson, J. Hietpas, and S. D. Samson (2013). “Likeness among detrital zircon populations—An approach to the comparison of age frequency data in time and space”. *GSA Bulletin* 125.11, pp. 1783–1799. doi: [10.1130/B30888.1](https://doi.org/10.1130/B30888.1).
- Saylor, J., D. Stockli, B. Horton, J. Nie, and A. Mora (2012). “Discriminating rapid exhumation from syndepositional volcanism using detrital zircon double dating: Implications for the tectonic history of the Eastern Cordillera, Colombia”. *Bulletin of the Geological Society of America* 124.5, pp. 762–779. doi: [10.1130/B30534.1](https://doi.org/10.1130/B30534.1).
- Sharman, G. R., J. P. Sharman, and Z. Sylvester (2018). “detritalPy: A Python-based toolset for visualizing and analysing detrital geochronologic data”. *The Depositional Record* 4.2, pp. 202–215. doi: [10.1002/dep2.45](https://doi.org/10.1002/dep2.45).
- Shimazaki, H. and S. Shinomoto (2010). “Kernel bandwidth optimization in spike rate estimation”. *Journal of Computational Neuroscience* 29.1, pp. 171–182. doi: [10.1007/s10827-009-0180-4](https://doi.org/10.1007/s10827-009-0180-4).
- Sundell, K. E. and J. E. Saylor (2021). “Two-Dimensional Quantitative Comparison of Density Distributions in Detrital Geochronology and Geochemistry”. *Geochemistry, Geophysics, Geosystems* 22.4, e2020GC009559. doi: [10.1029/2020GC009559](https://doi.org/10.1029/2020GC009559).
- Vermeesch, P. (2013). “Multi-sample comparison of detrital age distributions”. *Chemical Geology* 341, pp. 140–146. doi: [10.1016/j.chemgeo.2013.01.010](https://doi.org/10.1016/j.chemgeo.2013.01.010).
- (2018a). “Dissimilarity measures in detrital geochronology”. *Earth-Science Reviews* 178, pp. 310–321. doi: [10.1016/j.earscirev.2017.11.027](https://doi.org/10.1016/j.earscirev.2017.11.027).
- (2018b). “IsoplotR: A free and open toolbox for geochronology”. *Geoscience Frontiers. SPECIAL ISSUE: Frontiers in geoscience: A tribute to Prof. Xuanyue Mo* 9.5, pp. 1479–1493. doi: [10.1016/j.gsf.2018.04.001](https://doi.org/10.1016/j.gsf.2018.04.001).
- Villani, C. (2003). *Topics in Optimal Transportation*. American Mathematical Soc. 402 pp.